Atmos. Chem. Phys. Discuss.,
https://doi.org/10.5194/acp-2019-968-AC1, 2020

Atmospheric Chemistry and Physics Discussions

Interactive comment on "New eastern China agricultural burning fire emission inventory and trends analysis from combined geostationary (Himawari-8) and polar-orbiting (VIIRS-IM) fire radiative power products" *by* Tianran Zhang et al.

Tianran Zhang et al.

tianran.zhang@kcl.ac.uk

Received and published: 6 May 2020

We would like to thank the referee for his/her careful and thorough reading the manuscript and consider it is well written and relevant to ACP. Below are our responses to specific and technical comments.

 # 203 – it would be useful to outline the impact of the correction of grid cell FRP for cloud cover (i.e. the percentage FRP adjustment).

Response: We added following description:

"*Cloud cover (CC) fractions in some grid cells occasionally reach 0.5 (50%), but most are zero. After the cloud cover adjustment the mean FRP areal density across the study area increased by 11.5% , so the overall effect of the CC adjustment is relatively minor.*"

 # 225 and Figure 4 – the model fits the observed Himawari FRP well for most of the diurnal cycle although there is a reasonably strong secondary peak in fire activity around 20:00 which is not modelled. What is the impact of omitting the FRP contribution of this secondary peak to the daily FRE? (i.e. the difference between the 'modelled' Himawari FRP and the observed Himawari FRP). Figure 4 shows the 'summer' diurnal cycle. Are the observed Himawari diurnal cycles similar in shape in different seasons?

Response: The reason we do not model the secondary peak in daily FRE is that there is no satellite data from VIIRS available at this time of day to influence the peak magnitude. Instead of explicitly including this peak in the modelled diurnal cycle we include an FRP baseline above a zero value that is designed to make the daily FRE the same as if the secondary peak was modelled. This "baseline" methodology follows that of Andela et al. 2015 who used it for the same reason. To address the reviewers question we designed two simulations to compare this approach (Simulation 1) to that when the secondary peak is included (Simulation 2). In Simulation 1, the FRP derived from Himawari-8 at the VIIRS daytime and nighttime overpass times are used as ρ _peak and ρ _basein, whilst in Simulation 2 the distribution shown in Fig. 4 in our manuscript (red dots) is described as the sum of two Gaussian functions:

$$\widetilde{\rho}S2\left(t\right) = \sum \rho_{peaki} e^{-\frac{\left(h_t - h_{peaki}\right)^2}{2\sigma_i^2}}$$

Where σ_i from each peak i in Fig. 4 (2.39± 0.053 for σ_1 and 1.24± 0.12 for σ_2 during

June, 1.63$\pm$ 0.041 for σ_1 and 0.60$\pm$ 0.077 for σ_2 during October) are used here, h_{peaki} (h) is the hour in day when FRP reaches maximum for each of the peaks in the diurnal cycle (14.0 for h_{peak1} and 21.2 for h_{peak2} during June, 14.2 for h_{peak1} and 18.4 for h_{peak2} during October). The ρ_{peaki} are the daily Himawari-8 FRP observations at those two peak maximum times.

Results from these two simulations are shown in the Figure below, which has two time series covering 10th June to 15th June each. The upper time-series shows a comparison of the two simulations using the original FRP data from Himawari-8 and Simulation 1 (S1). S1 shows a slightly overestimated baseline on 10 June and underestimation of FRP near the second peak on 13 June. Meanwhile the lower timeseries is for Simulation 2 (S2), which shows better agreement with the original Himawari-8 FRP data on 13 June but a very slight overestimation on 11 June. However, the main purpose of including the diurnal cycle is to generate correct FRE daily values, so it is better to compare FRE totals from S1 and S2 rather than hourly FRP, and we do this in the Figure 1 of this comment below.

The summed daily FRP is here used to represent FRE (without the full temporal integration, Figure 2 of this comment). The scatterplots show a direct comparison of the summed daily FRP totals from S1 (blue, left) and S2 (green, right) as compared to those from Himawari-8. Comparisons are done for Summer (June) and Autumn (Oct). The slopes of the linear best fit to these data are 1.06 and 1.15 for S1 and S2 in June, and 0.97 and 0.94 in October, suggesting that S1 performs better in both June and October. The absolute differences of S1 and S2 compared to the "true" Himawari values are however always within 10% of each other. Therefore the impact of not including the 2nd diurnal cycle peak but representing this by a baseline instead is not considered highly significant.

The observed Himawari diurnal cycles look indeed similar in shape in different seasons except for the autumn main peak is smaller and second peak time is earlier (Figure 3 of this comment).

 # 302-310 – is the winter burning season (shown in Figure 5) detected in other emissions inventories (e.g. GFED and GFAS)? It would be useful to highlight the winter burning season in Figure 7. In relation to Figure 5, is there any difference in the proportion of day/night fire detections during the winter months?

Response: We have enhanced Figure 7 as the reviewer suggested, and we also demonstrate that this winter burning season was not detected by either GFED or GFAS.

We also investigate the day/night fire detections during summer/autumn/winter seasons and haven't observed significant difference among them. Figure 4 of this comment gives an example from year 2013.

 # $\sim$ 321 –What might be the cause in the reduction of amount of wheat residue burnt? The wheat yield in 2015 is marginally higher than it is in previous years (Table S1)?

Response: The authors believe that the most likely cause of the reduction in wheat residue burnt in 2015 compared to the prior two years is the introduction of a more aggressive policy with regards to banning agricultural residue burning. This was introduced by the local government in 2014 and was seen by us during fieldwork conducted in June 2014 and October 2015, with the latter seeing more restrictions and less burning. We also investigated yearly total FRP from MODIS Aqua in the 2003-2018 period in 30 provinces/cities (Figure 5 of this comment). We notice that most of the provinces and cities also show this pattern of a significant reduction in burning from 2015.

 # 354-359 – how do the agricultural emissions derived using this approach compare with those from Li et al., 2015

Response: The authors apologise here we used wrong citation in the manuscript, it should be the MIX inventory paper as below:

Li, M., Zhang, Q., Kurokawa, J.I., Woo, J.H., He, K.B., Lu, Z., Ohara, T., Song, Y., Streets, D.G., Carmichael, G.R. and Cheng, Y.F., 2015. MIX: a mosaic Asian anthropogenic emission inventory for the MICS-Asia and the HTAP projects. Atmos. Chem. Phys. Discuss, 15(23), pp.34813-34869.

In this paper, the authors stated that 'open biomass burning was considered as a natural emission source and excluded in the MIX inventory'. Therefore, we can only compare our emission to the listed four anthropogenic emissions in this study.

 # 459 – what are the combustion completeness values used in EO-derived emissions inventories such as GFED for residue burning?

Response: Leeuwen et al. (2014) was the source of combustion completeness (CC) values used within GFED. It reports that 'for crop residue CC, values ranged from 65 % for cotton and sugarcane and 85 % for wheat and bluegrass'. We use a CC value to convert our fuel consumption estimates into an estimate of the amount of dry matter that is actually set fire to in the fields. We assume a CC of what of 86% (Table S2) based on Huang et al., 2012, which is very close to the 85% assumed in GFED. So therefore our calculated "residue amount" is given by (fuel mass burned/0.86). This then is compared to the wheat yield data to give our "burning ratios" presented in Figure 10.

 # 482 – Are the DMB estimates for all crop types and were these calculated using the GlobalLand30 agricultural area estimates? How do these estimates compare to those from other studies?

Response: Yes, the DMB estimates in this study are for all crop types, and they were calculated using the GlobalLand30 landcover map for agricultural areas. We used the MIRCA2000 rotation cultivation dataset to identify which crop type was burning at a particular location at different times of year (Figure S1).

Figure 7 gives comparison of DMB reported in this paper compared to that of GFAS and GFED. We have generally higher estimates than GFAS/GFED thanks to the ability of the VIIRS sensor to identify far lower FRP fires (Zhang et al., 2017). Since agricultural residue fires are typically quite small and of low intensity, this ability significantly improves the overall estimate of DMB for these types of fires. Most regional crop residue burning estimates are based on the aforementioned "bottom up" crop yield-based approach and whilst they often do not report DMB estimates they do report CO2 emission estimates which are directly proportional to DMB because CO2 represents almost 95% of the carbon released. We already compare the CO2 emissions values from our methodology to those from the "bottom up" approach in Table 2.

 # 56 – 'this leads'

Response: Revised as suggested.

 # 63 – define MODIS

Response: Revised as suggested.

 # 65 – 'most BA'

Response: Revised as suggested.

 # 66- define GFED

Response: Revised as suggested.

 # 75 - define VIIRS

Response: Revised as suggested.

 # 210 – replace 'observed' with averaged

Response: Revised as suggested.

 # 223 – replace 'height' with magnitude

Response: Revised as suggested.

 # 237 – replace 'see below' with Equation 9

Response: Revised as suggested.

 # 248 and 252 – replace 'calculated' with estimated

Response: Revised as suggested.

 # 466 – replace 'most later researchers' with 'more recent research'

Response: Revised as suggested.

Figures

Figure 3 : Perhaps plot all of the data on the same graph and plot the data from the same day as that used in Figure 2.

Response: We have edited the plot as the referee suggests. Though the data from Himwari-8 is not available on the day used for this Figure 2 as the satellite was only launched some years later.

Figure 4 : Is the FRP diurnal cycle from all fires in Eastern China or just agricultural fires in the region?

Response: Agricultural fire is the dominant biomass burning in Eastern China, especially during burning season (accounts for over 99% of total FRP). We did include all the fires when calculating the FRP diurnal cycle. However, when we excluding those non-agricultural fires, the change to diurnal cycle is very limited. (Figure 6 of this comment). We got almost similar summer diurnal cycle σ value (2.40) compare to the one we use in this paper (2.39).

Figure 6 (and others): The density of map gridlines make it difficult to interpret the maps.

Response: We removed the gridlines and changed color theme to make the maps more readable.

Figure 8 – y-axis PM2.5 subscript

Response: Revised as suggested.

Interactive comment on Atmos. Chem. Phys. Discuss., https://doi.org/10.5194/acp-2019-968, 2020.

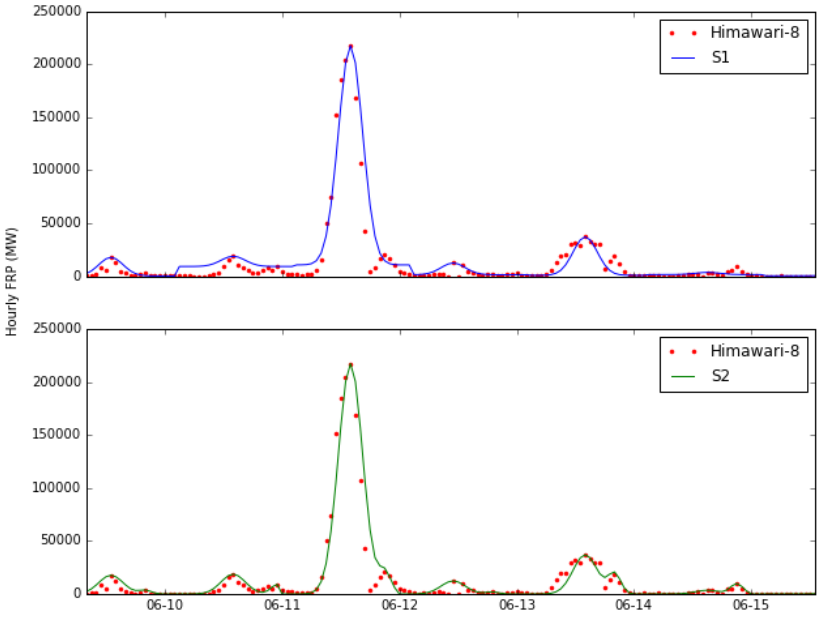
Himawari-8
S1
Himawari-8
S2
Hourly FRP (MW)
250000
200000
150000
100000
50000
0
06-10
06-11
06-12
06-13
06-14
06-15

Fig. 1.

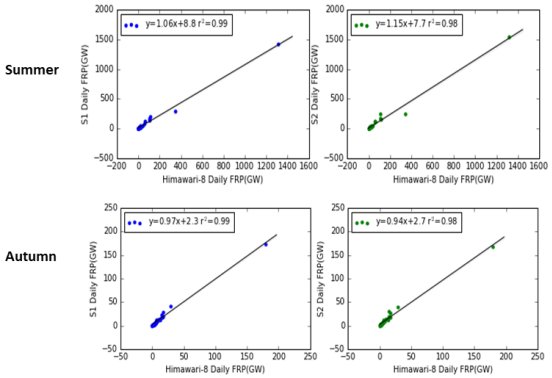
Summer
Autumn
y=1.06x+8.8 r²=0.99
y=1.15x+7.7 r²=0.98
y=0.97x+2.3 r²=0.99
y=0.94x+2.7 r²=0.98
S1 Daily FRP(GW)
S2 Daily FRP(GW)
Himawari-8 Daily FRP(GW)

Fig. 2.

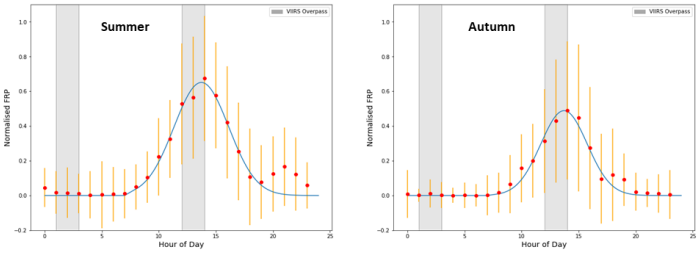
Summer
Autumn
VIIRS Overpass
Normalised FRP
Hour of Day

Fig. 3.

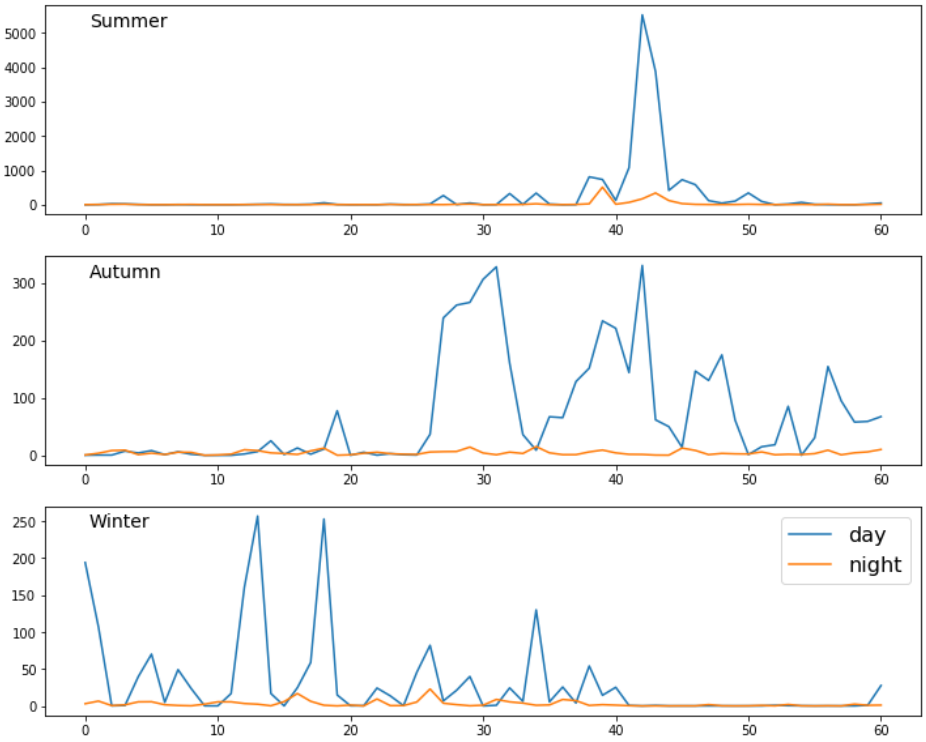
Summer
Autumn
Winter
day
night

Fig. 4.

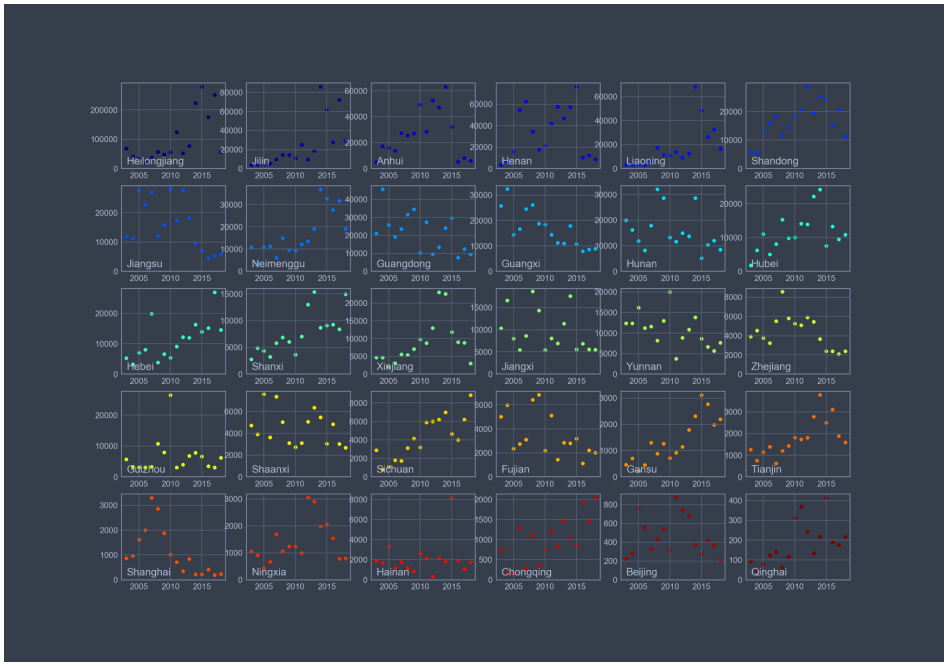
Heilongjiang
Jilin
Anhui
Henan
Liaoning
Shandong
Jiangsu
Neimenggu
Guangdong
Guangxi
Hunan
Hubei
Hebei
Shanxi
Xinjiang
Jiangxi
Yunnan
Zhejiang
Guizhou
Shaanxi
Sichuan
Fujian
Gansu
Tianjin
Shanghai
Ningxia
Hainan
Chongqing
Beijing
Qinghai

Fig. 5.

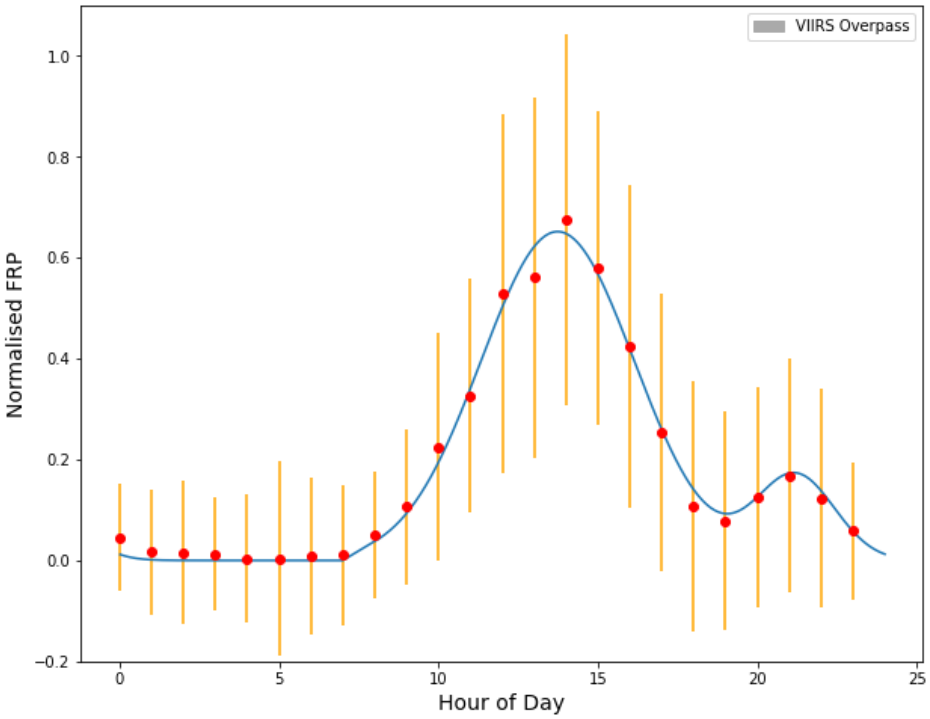
VIIRS Overpass
Normalised FRP
Hour of Day
1.0
0.8
0.6
0.4
0.2
0.0
−0.2
0
5
10
15
20
25

Fig. 6.